An all-silicon channel waveguide fabricated using direct proton beam writing

E. J. Teo[*a], A. A. Bettiol[a], M. B. H Breese[a], P. Y. Yang[b], G. Z. Mashanovich[b], W. R. Headley[b], G. T. Reed[b] and D. J. Blackwood[c]

[a] Centre for Ion Beam Applications, Department of Physics, National University of Singapore, 2 Science Drive 3, Singapore 117542

[b] Advanced Technology Institute, School of Electronics and Physical Sciences, University of Surrey, GU2 7XH, United Kingdom

[d] Department of Materials Science and Engineering, 7 Engineering Drive 1, National University of Singapore, Singapore 117574

ABSTRACT

We report a novel technique for the fabrication of an all-silicon channel waveguide using direct proton beam writing and subsequent electrochemical etching. A focused beam of high energy protons is used to selectively inhibit porous silicon formation in the irradiated regions. By over-etching beyond the ion range, the irradiated region becomes surrounded by porous silicon cladding. Waveguide characterization carried out at 1550 nm on the proton irradiated waveguide shows that the propagation losses improve significantly from 20±2 dB/cm to 9±2 dB/cm after vacuum annealing at 800°C for 1 hour.

Keywords: Proton beam writing, silicon photonics, porous silicon, waveguides

1. INTRODUCTION

Silicon is potentially the material of choice for optoelectronics and photonics integrated circuits due to its high transparency at the technologically important wavelengths of 1.3 and 1.55 µm. Furthermore, silicon photonics can benefit from the existing infrastructure available in the microelectronics industry thus allowing for monolithic integration of photonics and electronics onto a single silicon chip. Recently, there have been new initiatives to develop long wave infrared photonics integrated circuits for sensing and signal processing in the 3-5 and 8-14 µm atmospheric-transmission windows used in military, and also imaging and communications in the 30-100 µm terahertz regime.[1]

The most widely used platform for silicon photonics and waveguides is silicon-on-insulator (SOI) or more specifically silicon-on-silicon dioxide. This is due to the strong light confinement and low propagation loss that has been achieved for single mode waveguides (less than 1 dB/cm for rib and 2-3 dB/cm for strip waveguides) [2,3] With a high refractive index difference of 2 in the Si/SiO_2 waveguides, compact devices such as bends, splitters and ring resonators can be densely integrated into a single chip.[4-6] Conventional lithography and etching processes are used to define the SOI waveguides. One major problem of using SOI platform is the strong absorption of wavelengths in the range of 3.6-100 µm, limiting its application in the mid- and far-infrared regime.[1] New types of silicon-based waveguides structures such as photonic band gap silicon[7] and hollow core waveguides[8] have been developed to overcome this limitation.

* Corresponding author :Teo Ee Jin phytej@nus.edu.sg; Telephone:+65 65163507 Fax: +65 67776126

Silicon Photonics III, edited by Joel A. Kubby, Graham T. Reed
Proc. of SPIE Vol. 6898, 68980Q, (2008) · 0277-786X/08/$18 · doi: 10.1117/12.762771

In this paper, we demonstrate a method for fabricating all-silicon channel waveguides by utilizing a beam of keV protons and a single electrochemical etching step to produce a porous silicon (PSi) cladding. Previously, focused MeV protons have been used for applications in micromachining of high-aspect ratio structures and free-standing waveguides,[9,10]. Figure 1 shows the schematic diagram of the fabrication process. First, a highly focused beam of protons of 250 keV is used to write predefined patterns in silicon. As the ion penetrates the material, defects are created along the ion track, with most of the damage produced at the end of range. During the subsequent electrochemical etching process, these defects act to trap holes from migrating to the silicon/electrolyte surface, resulting in a significant reduction in the current flow through the damage region. This results in the formation of PSi in the unirradiated region. As the sample is etched beyond the depth of the ion range, the structure starts to become undercut due to the isotropic etching, resulting in the formation of a "mushroom" profile. Finally, the irradiated region is separated from the substrate and is surrounded by PSi. In a single etch step, it is possible to create a channel waveguide with PSi cladding. The core height is defined by the energy of the beam and the width by the scan parameters. This direct writing process eliminates the multiple processing of mask deposition and removal, allowing for quick prototyping of waveguides. According to Soref *et. al.*,[1] the Si/PSi waveguide system has a high transmittance in the ranges of 1.2-9 and 23-200 μm and is potentially important for mid and far-IR applications.

For this structure, light is confined in the silicon core by a PSi cladding. The advantage of using PSi is that it is compatible with standard silicon processes and easy to implement. More importantly, the thickness and refractive index can be tuned over a wide range of 1.2-3.0 by controlling the etching parameters.[11,12] Optical devices such as Fabry Perot microcavities and multilayer PSi waveguides have been produced using this approach.[11-14] This Si/PSi waveguide enables us to cover a wide range of refractive index differences from 0.5 to 2.3, that is normally achieved by using different systems and materials.[15] This has several implications on the waveguide properties, such as the bending radius and also single mode dimensions.[15] Very high index contrast can potentially be useful for making ultra-small and compact devices in integrated photonics circuits. Lower index contrast system can provide an alternative solution for reducing the losses due to scattering, and facilitating coupling from optical fibres.

Proton beam writing was carried using a Singletron accelerator at the Centre for Ion Beam Applications at the National University of Singapore.[16] A highly stable beam of 250 keV protons focused down to less than 60 nm, was used to irradiate a straight line across a p-type silicon wafer of 0.1 Ω.cm resistivity. Electrical contacts were made to the backside of the sample using In-Ga eutectic and copper wire, which is protected by epoxy. The sample was then etched electrochemically in a solution of hydrofluoric acid (48%) and ethanol with a ratio of 1:1 at a current density of 5 mA/cm^2 for 30 min. After etching, the sample was rinsed in ethanol and water for about 5 min.

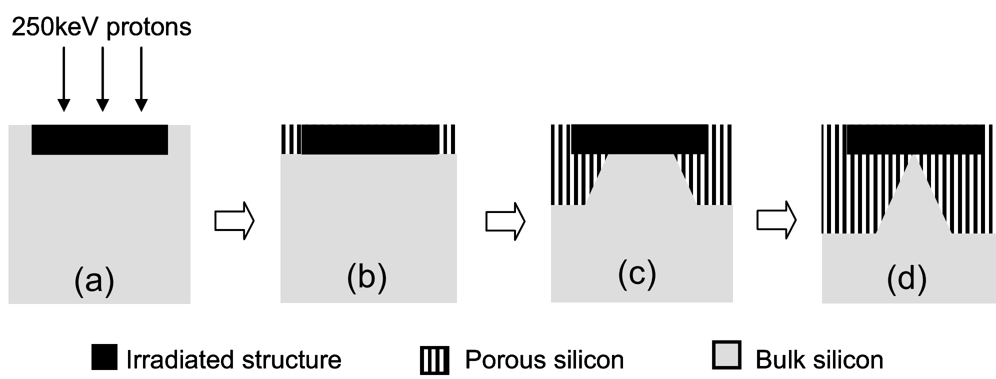

Figure 1. Schematic diagram of the waveguide fabrication process. (a) Proton beam writing in *p*-type silicon followed by (b) electrochemical etching in HF. (c) Prolong etching results in undercutting of the irradiated region and (d) finally it is surrounded by porous silicon.

3. Results and Discussions

The profile of the waveguides was observed using cross sectional scanning electron microscopy (SEM). To obtain a clean facet, the wafer was thinned down to about 200 μm, prior to cleaving. Figures 2 (a) and (b) show the top and cross sectional view of a waveguide structure irradiated with a dose of 1×10^{15} protons/cm^2. It has a width of 9.8 μm at the top and broadens to about 11.3 μm at the bottom as a result of higher deflection of the holes from the irradiated region at the end of range.[17] With an irradiation dose of 10^{15}/cm^2, the rate of PSi formation is reduced to almost zero in the irradiated regions and PSi is formed only in the unirradiated regions. The structure has a thickness of 2.4 μm, which corresponds to the penetration depth of 250 keV protons.[18]

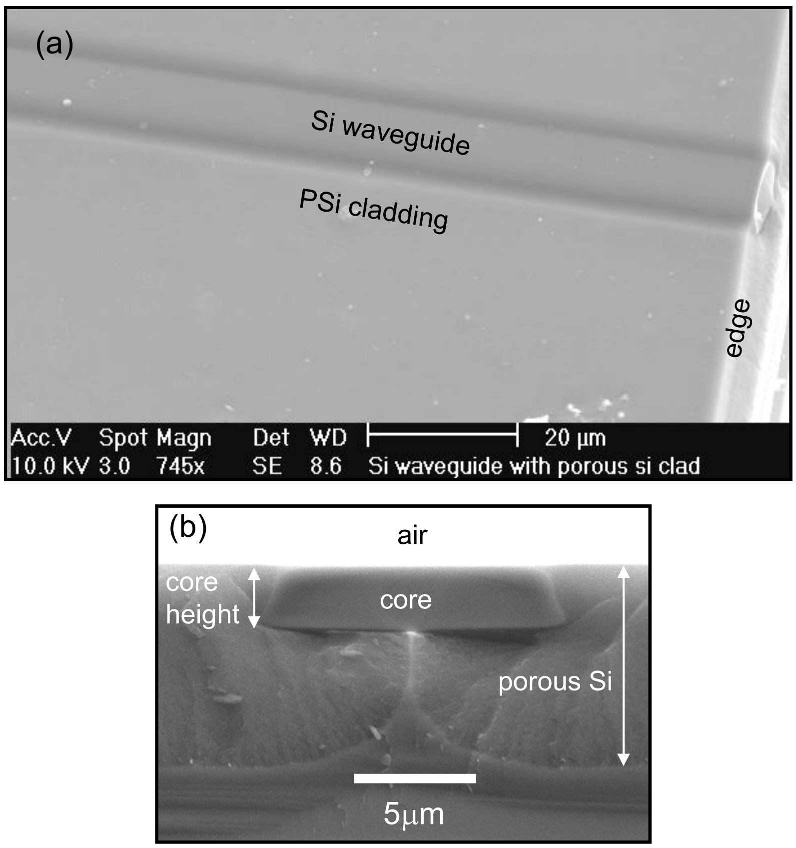

Figure 2. (a) Top and (b) cross sectional SEM view of the channel waveguide with PSi cladding.

The refractive index (n) of PSi is lower than that of bulk Si since it consists of air and silicon. We have used the Bruggeman formula[19] to simulate the effective dielectric function for PSi by fitting the reflectance spectra. The thickness of the PSi has been independently obtained using cross sectional SEM. The square root of the dielectric function resulting from the fit is the refractive index of the PSi. Figure 3 shows the reflectance spectra before and after annealing in Ar atmosphere at 800ºC for 1 hour. It is found that the refractive index is 1.55 before annealing and reduces to 1.48 after annealing. This change in refractive index is due to the partial oxidation of the porous silicon after Ar annealing. To prevent oxidation of the porous silicon, vacuum annealing has been used instead.

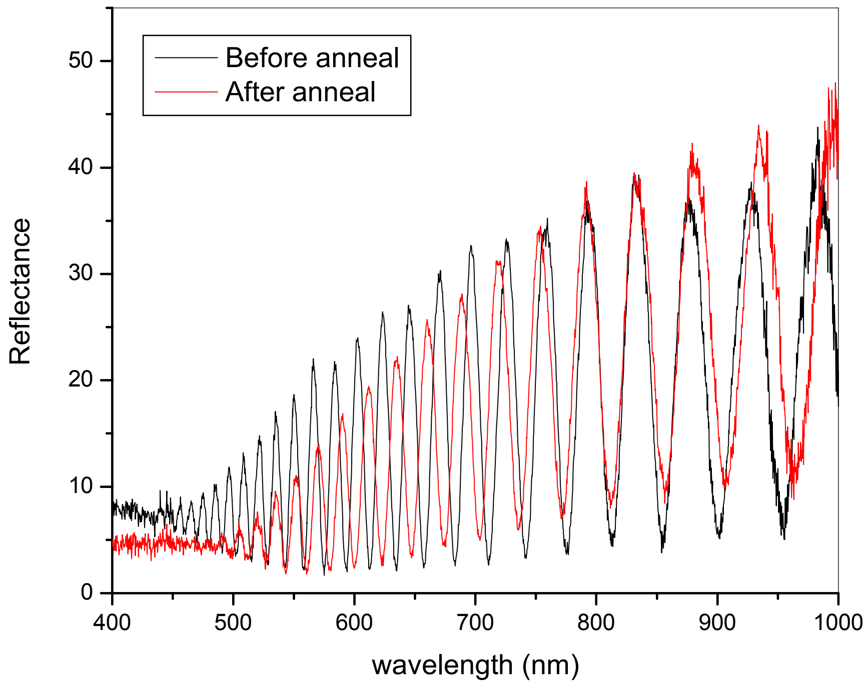

Figure 3: Reflectivity measurements of porous silicon before and after Ar annealing at 800ºC for 1 hour.

Optical characterization of the proton beam written waveguides is performed at a wavelength of 1550 nm. A 10 mW tunable infrared laser is coupled into the waveguide via optical fiber and the light output is imaged using a 50× objective lens and a videcon IR camera. Figure 4(a), (b) show the scattered light and output mode collected from the top and end of the waveguide respectively. Due to the large cross section, the light propagation is multi-mode and follows the profile of the waveguide. In order to determine the propagation loss in the channel waveguide, the scanning fiber technique is used whereby light scattered off the normal of the waveguide is detected using a sensitive power meter. This technique assumes that the intensity of the light propagating in the waveguide is proportional to the scattered light. Measurements are taken from the central part of the waveguide so that the effect of scattering off the edge of the sample can be minimized. To ensure the reproducibility of the loss values, measurements are taken over several times. The uncertainty in the loss is determined from the variations in the individual readings. Figure 4(c) shows a plot of the scattered light intensity in dB as a function of length along the waveguide. Our results show that the propagation loss of the irradiated waveguide is about 20±2 dB/cm. After annealing in vacuum at 800ºC for 1 hour, it is found that the losses reduce significantly to about 9±2 dB/cm. According to Day et. al.,[20] temperatures of 400ºC-450ºC are sufficient to anneal out more than 90% of the defects caused by proton irradiation in silicon.

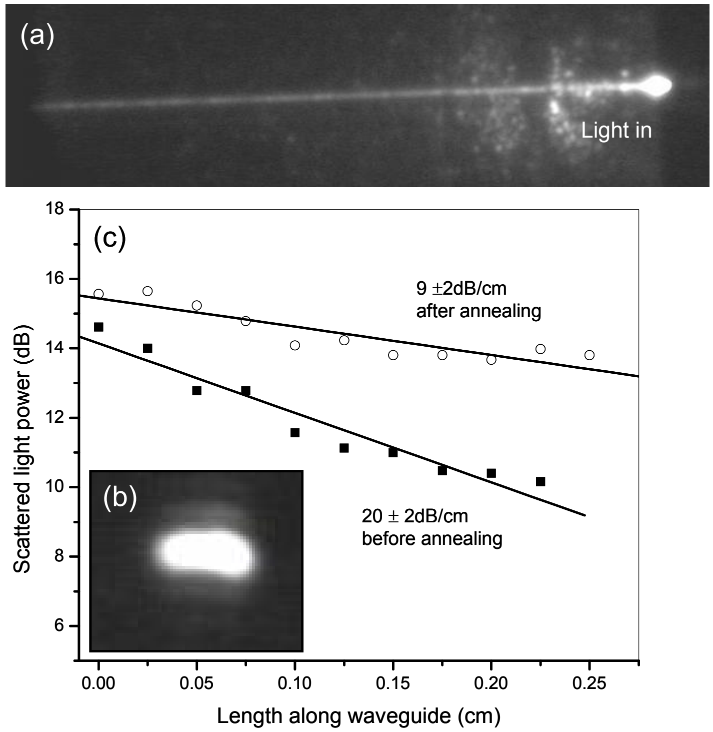

Figure 4. (a) Scattered light from the top of the waveguide, (b) output mode of the waveguide and (c) propagation loss measurement of silicon waveguide, before and after annealing at 800°C for 1 hour in vacuum. The scattered light power is defined as $10\log P_{out}$.

Although higher than commercially available SOI waveguides (< 1dB/cm), the losses are still lower than 7-50 dB/cm reported in PSi waveguides.[21,22] PSi based waveguides tend to suffer from scattering losses due to interface roughness formed at the PSi/Si front and Rayleigh scattering from the silicon nanocrystals.[23] Lerondel et. al.[24] showed that the interface roughness is largely dependent on the current density and viscosity of the HF and can be relatively high for low doped p-type silicon. This will have a detrimental effect on waveguides with high index contrast, since the scattering loss scales proportionally to $\Delta n^2 = (n^2_{core} - n^2_{clad})$.[25] Therefore, it is important to reduce the interface roughness to improve the loss. In our case, Rayleigh scattering will not be significant as the guiding medium used is silicon.

In order to determine the surface roughness of the waveguide, atomic force microscopy (AFM) is performed on the structure, after stripping the PSi layer with potassium hydroxide solution. In this case, the structure is etched for shorter time so that it is still firmly attached to the substrate. Figures 5 show the surface morphology of the unirradiated and irradiated structure. Although the unirradiated regions show a high surface roughness of about 20 nm root-mean-square (RMS) roughness, the top surface and sidewalls of the waveguide are much smoother with a RMS of 4.5 nm and 12.6 nm respectively. This is comparable with values of 10 nm in the sidewall roughness obtained by conventional lithography and etching technique.[26] The irradiation process also influences the sidewall morphology of the waveguide due to beam intensity fluctuations from the accelerator,[27] beam resolution and stage scanning speed.[28] Currently, we are investigating ways to reduce the surface roughness using different etching conditions and scanning parameters. Post-fabrication treatment such as oxidation and different annealing conditions will also be explored.

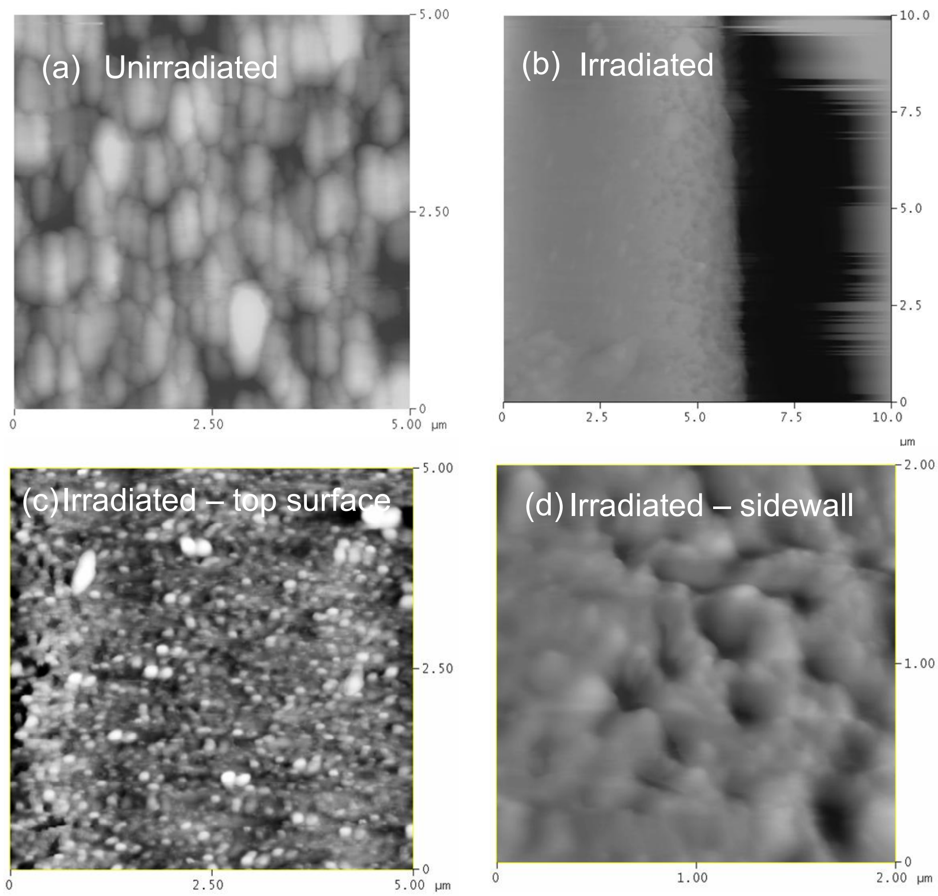

Figure 5: AFM image of the PSi/Si interface in the (a) unirradiated and (b) irradiated regions. Close-up view of the (c) top surface and (d) sidewalls of waveguide.

4. Conclusions

In conclusion, we have demonstrated the ability of direct proton beam writing and electrochemical etching for the fabrication of PSi clad waveguides in a single etch step. This technique gives us the flexibility to write any arbitrary patterns without the need for a mask, allowing quick prototyping of structures. Unlike conventional waveguide fabrication which uses SOI platform, the waveguide is fabricated entirely in silicon substrates and is suitable for mid-IR and far-IR applications. By controlling the refractive index of PSi, a wide range of refractive index contrast can be obtained in this type of waveguide. Our results are promising, showing a propagation loss of 9 dB/cm at 1550nm. This can be further improved by reducing the interface and sidewall roughness.

References

1. R. A. Soref, S. J. Emelett and W. R. Buchwald, J. Opt. A:Pure Appl. Opt. 8 840 (2006)
2. A.G. Rickman, G. T. Reed and F. Namavar, J. Lightwave Technol. 12 1771 (1994)
3. U. Fischer, T. Zinke, J.R. Kropp, F. Arndt, and K. Peterman, IEEE Photon. Technol. Lett., 8 647 (1996).
4. J. Foresi, P. Villeneuve, J. Ferrera, E. Thoen, G. Steinmeyer, S. Fan, J. Joannopoulos, L. Kimerling, H. Smith and E.Ippen, Nature 390 143 (1997)
5. T. Baehr-Jones, M. Hochberg, C. Walker, A. Scherer , Appl. Phys. Lett. 85 3346 (2004).
6. T. Tsuchizawa, K. Yamada, H. Fukuda, T. Wantanabe, J. Takahasi, M. Takahashi, T. Shoji, E. Tamechika, S. Itabashi and H. Morita, IEEE J. Quantum Electron. 11 232 (2005)
7. S. W. Leonard , H. M. van Driel, A. Birner, U. Gosele, P. R. Villeneuve, Opt. Lett. 25 1550 (2000)
8. R. Bernini, S. Campopiano and L. Zeni, IEEE J. Quantum Electron. 8 106 (2002)
9. E. J. Teo, M. B. H Breese, E. P. Tavernier, A. A. Bettiol and F. Watt, M. H. Liu and D. J. Blackwood, Appl. Phys. Lett., 84 3202 (2004)
10. P. Yang, G. Mashanovich , E. J. Teo , M. B.H. Breese , I. Gomez-Morilla , W. Headley, D.J. Blackwood , A.A. Bettiol , G.T. Reed, Appl. Phys. Lett. 90 241109 (2007)
11. L. Pavesi, Riv. Nuovo Cimento 10, 1 (1997)
12. M. G. Berger, R. Arens-Fisher, M. Thonissen, M. Kruger, S. Billat, H. Luth, S. Hilbrich, W. Theiss, and P. Grosse, Thin Solids Films 297 237 (1997).
13. M. Araki, H. Koyama, and N. Koshida, Appl. Phys. Lett. 69, 2956 (1996).
14. S. Nagata, C. Domoto, T. Nishimura, and K. Iwameji, Appl. Phys. Lett. 72, 2945 (1998).
15. A. Melloni, R. Costa, G. Cusmai, F. Morichetti and M. Martinelli, Proc 2005 IEEE/LEOS Workshop on Fibres and Optical Passive Components, 246, June 2005.
16. F. Watt, A. A. Bettiol, J. A. van Kan, E. J. Teo and M. B. H. Breese, Int. J. Nanoscience 4 269 (2005)
17. M.B.H. Breese, F.J.T. Champeaux, E.J. Teo, A.A.Bettiol and D. Blackwood, Phys. Rev. B 73 035428 (2006)
18. J. F. Ziegler, J. P. Biersack, U. Littmark, in The Stopping and Range of Ions in Solids, (Pergamon Press, New York 1985).
19. A. A. G. Bruggeman, Ann. Phys. 24 636 (1925)
20. Day A. C., Horne W. E. and Arimura I, IEEE Trans. Nucl. Sci. 27 1665 (1980)
21. H. F. Arrand, T. M. Benson, P. Sewell, A. Loni, R. J. Bozeat, R. Arens-Fischer, M. Kruger, M. Thonissen and H. Luth, IEEE J. Quantum Electron. 4 975 (1998)
22. G. Amato, L. Boarino, S. Borini and A.M. Rossi, phys. stat. sol. A 182 425 (2000)
23. Ferrand P., Romestain R., Appl. Phys. Lett. 77 3535 (2000)
24. Lerondel G. Romestain R and S. Barret, J. Appl. Phys. 81 6171 (1997)
25. P. K. Tien, Appl. Opt. 10 2395 (1971)
26. K. K. Lee, D. R. Lim, L. C. Kimerling, J. Shin and F. CerrinaOpt. Lett. 26 1888 (2001)
27. E. J. Teo, M.B.H. Breese, A. A. Bettiol, F. Watt L. C. Alves, J. Vac. Sci. Technol. B 22 560 (2004)
28. T. C. Sum, A. A. Bettiol, H. L. Seng, J. A. van Kan, and F. Watt, Appl. Phys. Lett. 85 1398 (2004)